

EFFECT OF DARK MATTER HALO SUBSTRUCTURES ON GALAXY ROTATION CURVES

NIRUPAM ROY

NRAO, P. O. Box O, 1003 Lopezville Road, Socorro, NM 87801, USA

Accepted for publication in ApJ

ABSTRACT

The effect of halo substructures on galaxy rotation curves is investigated in this paper using a simple model of dark matter clustering. A dark matter halo density profile is developed based only on the scale free nature of clustering that leads to a statistically self-similar distribution of the substructures at galactic scale. Semi-analytical method is used to derive rotation curves for such a clumpy dark matter density profile. It is found that the halo substructures significantly affect the galaxy velocity field. Based on the fractal geometry of the halo, this self-consistent model predicts an NFW-like rotation curve and a scale free power spectrum of the rotation velocity fluctuations.

Subject headings: dark matter — galaxies: dwarf — galaxies: general — galaxies: ISM — galaxies: structure — ISM: kinematics and dynamics

1. INTRODUCTION

Observational and theoretical studies of galaxy rotation curves (Rubin & Ford 1970), velocity dispersions of elliptical galaxies (Faber & Jackson 1976), baryon fraction in clusters (Clowe et al. 2006; Massey et al. 2007), gravitational lensing, structure formation, CMB power spectrum etc. indicate that a significant fraction of the mass of the Universe has no electromagnetic interaction (Bertone et al. 2005). At galactic scale, the main evidence for the existence of such gravitating matter with very high mass to light ratio comes from observations of galaxy rotation curves. The gravitational potential derived from the observed rotation curve can not be explained only by the visible mass with any reasonable mass to light ratio (Rubin & Ford 1970, 1980; Sofue 1996; Sofue & Rubin 2001; Spano et al. 2008). Though there are modified theories of the gravitation and other suggestions (Milgrom 1983; Bekenstein & Milgrom 1984; Sanders 1986; Fahr 1990; Sanders 1997; Brownstein & Moffat 2006) to explain this anomaly, the dark matter concept is widely accepted to be a simpler explanation of these observations. Though observations of galaxy rotation curves established the existence of the dark matter at galactic scale, there is no general agreement on the nature and various properties (like mass distribution) of this major constituent of the Universe (Navarro et al. 1996; de Blok 2005). Potentially, galaxy rotation curves can also shed light on some aspects of the dark matter properties and thus help us in deriving a better understanding of the nature of the dark matter. One such key aspect is the density profile or the mass distribution of the dark matter at galactic scale.

On the theoretical front, there are various mass distribution models of the dark matter halo. The isothermal profile, the Navarro-Frenk-White (NFW) profile and some variant of these two profiles are used extensively in both theoretical and observational studies. An almost flat observed rotation curve outside the core of a galaxy led to the dark matter halo model with $1/r^2$ isothermal density profile (Begeman et al. 1991; Burkert 1995).

The density at the centre is not finite in this model. However, it is possible to impose appropriate boundary conditions to derive a non-singular solution with density $\rho(r)_{NIS} = \rho_0 r_c^2 / (r_c^2 + r^2)$, where ρ_0 is the central density and r_c is the “core radius”. At large radius, this profile will be similar to $1/r^2$ singular isothermal profile. A cut-off radius r_{max} is also required to be imposed to keep the total mass of the halo finite. However, the non-singular isothermal profile was not very successful in explaining the observed rotation curves. A significant progress in the field was the introduction of an alternative density profile, the NFW density profile, $\rho(r)_{NFW} = \rho_0 r_c^3 / [r(r_c + r)^2]$, where ρ_c and r_c are the characteristic density and characteristic radius respectively (Navarro et al. 1996, 1997; Jing 2000).

The NFW profile has been quite successful in explaining the observed rotation curves for many galaxies. Over the time, a class of variant of the isothermal and the NFW profiles are also introduced to fine tune the agreement of theory and observations (Burkert 1995; Zhao 1996; Fukushige & Makino 2001). All these density profiles are of more or less similar merit, as far as explaining the rotation curve is concerned. However, detailed analysis shows that the NFW profile has a number of problems. For example, observations of galaxies and clusters suggest a central flat density core (de Blok 2007; Kuzio de Naray et al. 2008), whereas, in NFW profile, dark matter density has a central cusp with a logarithmic slope ≈ -1 . Numerical simulations show that the presence of baryon can change the mass distribution significantly (El-Zant et al. 2004; Shlosman 2010, and references therein), and for isothermal cusp, minor merger and dynamical friction may lead to a shallower central density slope (Romano-Díaz et al. 2008). The NFW profile also seems not to fit the observed rotation curves of the dark matter dominated low surface brightness galaxies and low mass dwarf galaxies (de Blok 2002, 2005). A more serious issue with the NFW profile is that the profile is derived by fitting analytical function to the density distribution derived from numerical simulation of structure formation with dark matter. This, in a sense, lacks a proper physical understanding. Though some physical insight of the NFW profile have recently

come from further high resolution dark matter simulations (e.g., Taylor & Navarro 2001), the issue is far from being settled. Moreover, even if these cosmological simulations are very successful on large scale, at galactic scale there are unsolved issues, like the “angular momentum problem” (Sommer-Larsen, Gelato & Vedel 1999; Sommer-Larsen & Dolgov 2001; Burkert & D’Onghia 2004) or the “missing satellite problem” (Klypin et al. 1999; Moore et al. 1999), which are yet to be addressed.

Here, we have developed a self-consistent model of the dark matter halo substructure distribution at galactic scale to explain observed NFW-like rotation curves. Support for the existence of dark matter substructures has mainly come from numerical simulations (Giocoli et al. 2008; Madau et al. 2008; Springel et al. 2008; Elahi et al. 2009a; Ludlow et al. 2009). But, there are strong observational hints like flux anomalies and time delays in gravitational lensing (Chen 2009; Keeton & Moustakas 2009; Vegetti & Koopmans 2009; Xu et al. 2009), or enhanced gamma rays and leptonic cosmic rays (Elahi et al. 2009b; Pinzke et al. 2009), indicating the presence of substructures. The present model is based on the assumption of a scale free nature of the dark matter clustering that leads to a statistically self-similar distribution of the halo substructures at galactic scale. It is shown that a simple fractal model of the dark matter halo substructure predicts an NFW-like rotation curve. Such a model also predicts a scale free power spectrum of the rotation velocity fluctuations. The model is described in Section 2, and the results are presented in Section 3. Possible limitations of our analysis are discussed in Section 4. Finally, we summarize and present our conclusions in Section 5.

2. THE MODEL

2.1. Assumptions, Parameters and Constraints

Assuming that the dark matter clustering has a scale free nature (i.e., there exist halo substructures of a wide range of mass), the density profile can be described as a combination of a smooth radial profile $\rho(r/r_c)$ and a stochastic part $\delta\rho$. Here r_c is a characteristic “core” radius and $\bar{\rho}$ contains information of the density variation at scales larger than or comparable to r_c . For the purpose of this work, we have used a simpler model of this density distribution which, however, retains all relevant key features. In this simplified model, we have assumed that each dark matter clump has a number of smaller clumps around it. Each of these smaller clumps are in turn just a scaled down version with even smaller clumps around them. As a result, the whole structure has an approximate spherical symmetry and a statistical self-similarity. It is assumed here that all these clumps have non-singular isothermal density profile where the central density (ρ_0), the core radius (r_c), the cut-off radius (r_{max}) and the halo to subhalo distance (D) are scaled down accordingly. However, this specific density profile is not a crucial assumption in our model and the individual substructures may have any non-singular density profile $\rho(r/r_c)$, where r_c is some characteristic radius. Essentially, this is a fractal structure with three parameters: (i) n , the number of small clumps around any clump, (ii) f_r , spatial scaling factor for core radius, cut-off radius and distance and (iii) f_ρ , central density scaling factor between any clump and its next smallest

clumps. A fractal is a fragmented and irregular geometrical shape with exact or stochastic self-similar structures at all scales (Mandelbrot 1983). Independent of the value of f_r and n , the (Hausdorff) fractal dimension of such a structure is 3 for $nf_r^3 < 1$. However, since at each iteration, the linear size of clumps scales by a factor f_r and the mass scales by a factor n , the local mass dimension for any substructure level is $D_m = -\log(n)/\log(f_r)$ over a certain range of scales. A mass dimension of D_m for a medium implies that the mass enclosed in a sphere of radius r in such a medium will be $M(r) = kr^{D_m}$. So, for the N^{th} substructure level, $M_N(r) = k_N r^{D_m}$ over a range of scales depending on N , n , f_r , D and r_{max} . Note that this range is different for different substructure levels. Hence, for the complete structure, the total mass $M(r)$, which is the sum of $M_N(r)$ of all the substructure levels, will not have a simple power law radial dependence. But, the dark matter halo mass function will still be a power law, $N(m) \propto m^{-\alpha}$, where the power law index $\alpha = -\log(n)/\log(f_r^3 f_\rho)$ is a more physically motivated parameter of this model and can be constrained from theoretical and numerical analysis of dark matter structure formation (Gao et al. 2004; Zemp et al. 2009). The density distribution can be written as

$$\rho(r) = \rho_{bg} + \sum_{i=0}^{\infty} \sum_{j=1}^n \rho_s(\rho_{0,i}, r_{c,i}, r_{max,i}, \vec{r}_{i,j}) \quad (1)$$

where ρ_{bg} is background density and $\rho_s(\rho_{0,i}, r_{c,i}, r_{max,i}, \vec{r}_{i,j})$ is density profile of individual substructure centred at $\vec{r}_{i,j}$ with central density ($\rho_{0,i}$), core radius ($r_{c,i}$) and cut-off radius ($r_{max,i}$). Considering the self-similarity of this model,

$$\begin{aligned} \rho_{0,i} &= f_\rho \times \rho_{0,i-1} \\ r_{c,i} &= f_r \times r_{c,i-1} \\ r_{max,i} &= f_r \times r_{max,i-1} \\ \vec{r}_{i,j} &= \vec{r}_{i-1,k} + (f_r \times D_{i-1} \times \vec{d}) \end{aligned} \quad (2)$$

where $k = n^{i-1}$, \vec{d} is a unit length vector with random orientation and the initial set of parameters $\rho_{0,0}, r_{c,0}, r_{max,0} = \rho_0, r_c, r_{max}$ is for the largest subhalo centered at the origin. In principle, ρ_{bg} may be a smooth function of r . But, since we are assuming it to be a small background density threshold, its effect on the final rotation curve is not very significant. So, for simplicity, we have assumed ρ_{bg} to be constant over the radius of our interest. This structure is shown schematically (without any randomness for the sake of clarity) in the left panel of Figure 1. After introducing randomness in angular position of the subhalos, one realization of such a structure with $n = 7$ and $f_r = 0.33$ is shown with two and four substructure levels in the middle and right panel respectively. This model can be considered as a simplified representation of the scale free, clumpy density structure of dark matter above a small threshold density at the galactic scale.

We note that the parameters for this model are constrained to a good extent by various physical considerations. Assuming that the structure is extended down to the infinitely small scale, to avoid a divergence of the total mass, the quantity $nf_r^3 f_\rho$ must be less than unity. Similarly, for a halo with cut-off radius r_{max} , halo

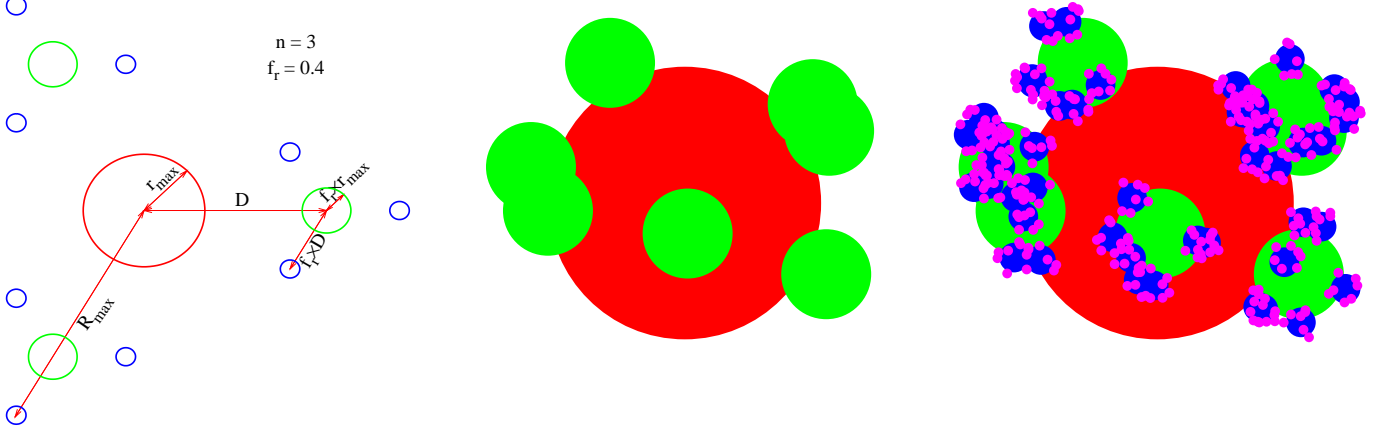


Figure 1. *Left:* Schematic representation of the halo substructure with three subhalos around any big halo. Note that both the cut-off radius (r_{max}) and the halo to subhalo distance (D) are scaled down by a factor f_r for each substructure level. *Middle and Right* Halo substructure with seven subhalos around any big halo and with $f_r = 0.33$. The middle and right panels show the structure with two and four substructure levels respectively.

to subhalo distance D must be greater than or equal to $(1 - f_r)r_{max}/(1 - 2f_r)$ to avoid any overlap. Also note that the density of any subhalo at the cutoff radius $\rho(r_{max})$ scales as f_r^3 . So, we adopt $f_r = 1.0$ for further analysis to ensure a constant density at the cutoff radius for all the substructures. In this simplified model, we have assumed that all the parameters like D , ρ_0 , r_{max} etc. are identical for all the subhalos for a particular substructure level and n , f_r and f_r^3 remain constant for all the levels. In a realistic situation, however, all these parameters may have some random variation. As a result of these fluctuations, the halo mass function, the radial mass distribution, and in turn, the rotation curves, are expected to be somewhat smoother than that are predicted from this analysis.

2.2. Tidal stability

A much stronger constraint on the parameters comes from the consideration of the stability of this structures preventing tidal disruption by invoking self-gravity. Considering a rigid object of mass m and radius r at a distance d from a bigger object of mass M and radius R , from the standard Roche limit consideration, D should be $\sim r(2M/m)^{1/3}$ to avoid tidal disruption of the smaller body. In the case of any halo and its immediate subhalo, $m/M = f_r^3$ and $r/R = f_r$ imply $d \approx 1.25R$. For even smaller subhalo structures with $r/R = f_r^k$, the mass is scaled accordingly $m/M = f_r^{3k}$ and $d \approx 1.25R$ assures stability. Hence, a distance

$$D \geq 1.25x \frac{1 - f_r}{1 - 2f_r} r_{max} \quad (3)$$

will make the whole structure stable. Here x is a fudge factor and we use the value of $x = 1.1$ to accommodate non-rigid density clumps. For a given value of D , the number of substructure n is also constrained to be

$$n \leq \frac{4\pi D^2}{\pi(f_r D / (1 - f_r))^2} = \frac{4(1 - f_r)^2}{f_r^2} \quad (4)$$

to avoid any possible overlap of subhalo structures.

2.3. Virial stability

A detailed virial stability analysis requires numerical simulation of the dynamics of such a density distribution to get the time-averaged dynamical quantities. But, a simple ensemble average virial scaling analysis may be used to constrain the central density ρ_0 for a set of model parameter. As the whole structure is assumed to have an approximate spherical symmetry, average kinetic and potential energies, $\langle T \rangle$ and $\langle V \rangle$, for thin spherical shells of radius r and thickness δr will be

$$\begin{aligned} \langle T \rangle &= \frac{1}{2} m \sigma_{DM}^2 = \frac{1}{2} 4\pi r^2 \delta r \rho(r) \sigma_{DM}^2 \\ \langle V \rangle &= -\frac{GM(r)m}{r} = -v_c^2(r) 4\pi r^2 \delta r \rho(r) \end{aligned} \quad (5)$$

where σ_{DM} is dark matter velocity dispersion, $M(r)$ is total mass within radius r and $v_c(r) = (GM/r)^{1/2}$ is the scale dependent virial velocity equivalent of the “circular velocity” for rotating disk. Since the rotation curve has a roughly constant value v_0 at large radius, the ratio $2\langle T \rangle / |\langle V \rangle|$ will tend to the equilibrium value of 1 at large radius if $\sigma_{DM} \approx v_0$. Using the minimum value for D from equation (3), the maximum extent of the structure R_{max} will be $D/(1 - f_r)$ and the average density will be

$$\langle \rho \rangle = \frac{3(1 - 2f_r)^3 (s - \tan^{-1}s)}{(1.25xs)^3 (1 - nf_r^3)} \rho_c \quad (6)$$

where $s = r_{max}/r_c$. Note, however, that this is a fractal structure with significant porosity. So, the average density of any individual clump is higher than $\langle \rho \rangle$ by a factor of $(1 - nf_r^3)(R_{max}/r_{max})^3$. Now, for global stability of the whole structure, R_{max} should be less than or equal to the radius within which the virial equilibrium is maintained. Average density within this virial radius r_{vir} or r_{200} should be ≈ 200 times more than the critical density $\rho_{crit} = 3H^2/8\pi G$. For a choice of model parameters n , f_r , s and x , this will constrain the lower limit of the central density ρ_0 so that $\langle \rho \rangle \gtrsim 200\rho_{crit}$. For individual substructures, both mass and volume scale as f_r^3 , keeping the average density constant. This implies that stability for one substructure level ensures stability for all other levels.

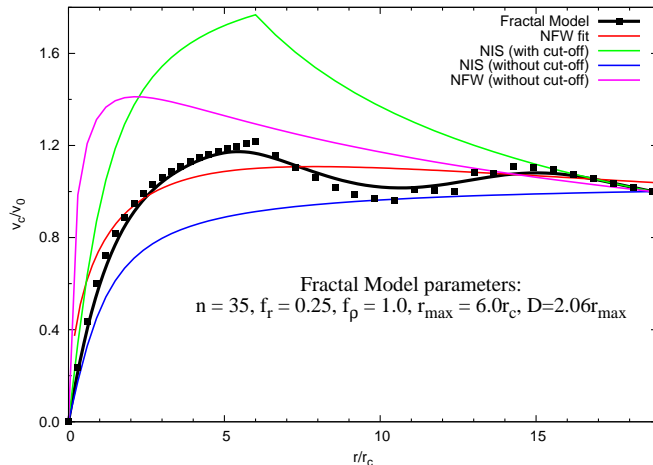


Figure 2. Predicted rotation curve for the fractal substructure model (black) and the best fit NFW profile to that (red). This is for $n = 35$, $f_r = 0.25$, $f_\rho = 1.0$ and $r_{max} = 6.0r_c$. Rotation curves for non-singular isothermal sphere with and without a cut-off (green and blue curves respectively) as well as for NFW halo (magenta curve) are also shown for a comparison. Radial distance and rotation velocity are scaled by r_c and v_0 (rotation velocity at the furthest radial distance) respectively.

3. RESULTS

3.1. Rotation curve

Since the halo density distribution is significantly clumpy, the velocity field for such a system is also expected to have fluctuations at all scales. However, due to approximate spherical symmetry of the clump distribution, the average rotation velocity over a spherical shell at radius r will still be $\langle v_c(r) \rangle \approx (GM_r/r)^{1/2}$, where M_r is the total mass within this radius. As pointed out in subsection 2.3 using the virial stability argument, the virial velocity or, equivalently, the “rotation” velocity is expected to be approximately same as the local velocity dispersion. This derived rotation curve for the fractal model is found to be NFW-like at large radial distance. At small radius, by construction, the rotation curve is obviously exactly same as that of a non-singular isothermal halo. This is shown in Figure 2. Radial distance is scaled by r_c and rotation velocity is scaled by v_0 , which is the rotation velocity at the maximum radius plotted. The black curve is the predicted rotation curve for the fractal substructure model with $n = 35$, $f_r = 0.25$, $f_\rho = 1.0$ and $r_{max} = 6.0r_c$ and the red line is the best fit NFW profile to that. The background density threshold ρ_{bg} is assumed to be negligible in this model. Rotation curves for non-singular isothermal sphere with and without a cutoff (green and blue curves respectively) as well as for NFW halo (magenta curve) are also shown in Figure 2 for a comparison. The velocity scaling ensures that the total mass encompassed by the maximum radius is same for all models.

The effect of the background density threshold ρ_{bg} is shown in Figure 3. Here, the rotation curve is evaluated for different ρ_{bg} keeping all other parameters same as in Figure 2. For scaling, we have used the density $\rho(r_{max})$ at the cutoff radius $r_{max} = 6.0r_c$. Different curves in Figure 3 are for $\rho_{bg}/\rho(r_{max}) = 0.00, 0.03, 0.10$ and 0.30 (black, red, green and blue curve respectively). The gen-

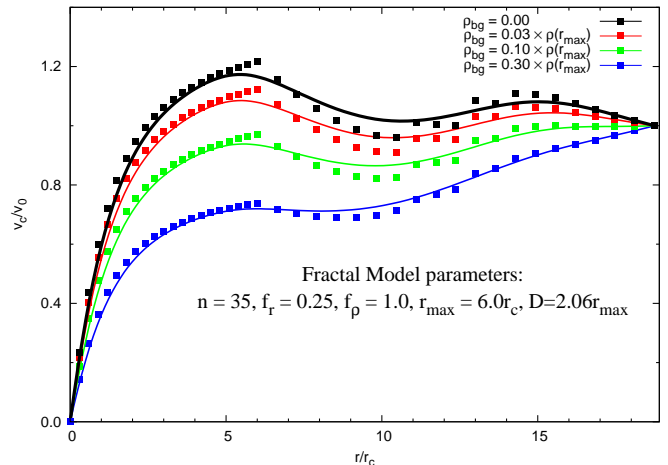


Figure 3. Predicted rotation curve for the fractal substructure model for different background density threshold ρ_{bg} . All other parameters are same as in Figure 2. Different curves are for $\rho_{bg}/\rho(r_{max}) = 0.00, 0.03, 0.10$ and 0.30 (black, red, green and blue curve respectively).

eral NFW-like nature of the rotation curve and the radial fluctuations remain unchanged. But depending on the value of ρ_{bg} , rotation curve at large radius may be rising, flat or declining. Note that the derived rotation curves shown in Figure 3 are with the simple model of a constant ρ_{bg} . In reality, ρ_{bg} is expected to be decreasing with increasing r , giving rise to a rotation curve somewhat intermediate between the extremes shown in Figure 3.

3.2. Velocity fluctuations

The predicted rotation curve due to the clustering of dark matter subhalos is very similar to the observed rotation curve and the empirical NFW rotation curve. However, unlike the NFW model with a smooth radial density distribution, the present model predicts a significant fluctuation of rotation velocity in both angular and radial directions. Since the underlying density field, which gives rise to this velocity fluctuations, is scale free, the velocity fluctuation power spectrum is expected to be a power law. Though the fractal model has many free parameters, the only relevant parameters for the index of this power law are n and f_r while the rest of them will just introduce different multiplicative scaling. This prediction can be easily verified from high spatial and spectral resolution observation of neutral hydrogen of normal galaxies. Note that part of this fluctuations will cancel out for the spherically averaged rotation curve and hence it is important to use the full velocity field to search for such scale free fluctuations. It is also important to note that fluctuations of the velocity field of the hydrogen gas will have contributions from the local density perturbations of the disk. But the scale dependence of these perturbations may makes it possible to disentangle the scale free perturbations due to the halo substructures. There is some indication of such a power law scaling of the rotation velocity fluctuation power spectra from direct observation and analysis of the H I 21 cm velocity field of some nearby galaxy (Dutta et al. 2010). We leave a more detailed treatment of this aspect to a future work.

4. DISCUSSION

Throughout this analysis we have assumed that the clump distribution in this model has an approximate spherical symmetry. This assumption is most likely to be untrue in reality. Due to small count, bigger substructures are more likely to cause departure from spherical symmetry. In this situation, rotation velocity field will also have strong azimuthal asymmetry. Observationally, about half of the spiral galaxies show some degree of kinematical lopsidedness (Richter & Sancisi 1994; Haynes et al. 1998; Swaters et al. 2008; Sofue & Rubin 2001; Jog & Combes 2009) which may originate from tidal distortion partly due to deviation from spherical symmetry of the underlying gravitational potential of the lopsided dark matter halo (Chakrabarti & Blitz 2009; Saha et al. 2008). Due to their large number, smaller substructures are likely to have relatively more symmetrical distribution. So, the velocity fluctuations spectrum is expected to show a power law scaling at large spatial frequency (large k , i.e., small physical scale), and a departure from power law at small k .

We have also assumed in this analysis that the baryons will not significantly affect the galactic dynamics. However, some recent numerical studies (e.g. Weinberg et al. 2008; Romano-Díaz et al. 2008, 2009) have shown that the presence of baryons have effects like flattening the central cusp, reducing the halo triaxiality, and introducing bias in clustering with environment density. Effectively, baryon dissipation may destroy the similarity between different scales of clustering. However, Romano-Díaz et al. (2010) have found that phenomenon like “efficient feedback from stellar evolution and the central supermassive black holes” may counterbalance this effect to some extent. On the other hand, Knebe et al. (2010) have found no significant effect of baryonic physics on properties like shape and radial alignment of substructures. Numerical simulations also suggest that, even in the presence of baryons, the subhalo mass function remains a power law though the power law index changes from -0.99 to -1.13 (Romano-Díaz et al. 2010). It is, hence, important to keep in mind that, in a realistic situation, baryon dissipation may alter the velocity fluctuations causing a significant departure from the scale free velocity fluctuations.

We note that the key result of this analysis, that is an NFW-like rotation curve for the fractal model, is not crucially dependent on the exact density profile of individual halos. A variety of density profile without any central singularity (variant of non-singular isothermal sphere) will lead to a similar NFW-like rotation curve. This strongly suggests that the clustering properties of the dark matter particles dominantly govern the radial density profile of the halo. Finally, these assembly of substructures will give rise to a flat NFW-like rotation curve for normal galaxies. But, for more dark matter dominated low mass dwarf galaxies and low surface brightness galaxies, depending on the exact form of the non-singular density profile, the dominant contribution of the central big halo may make the rotation curve for such galaxies intrinsically different which is consistent with observational results (de Blok 2002, 2005).

5. CONCLUSIONS

1. The dark matter halo substructures at galactic scale is found to significantly affect the rotation curve.
2. A self-consistent model of statistically self-similar hierarchical dark matter substructures predicts an NFW-like rotation curve, though each clump has a non-singular isothermal density profile. This NFW-like rotation curve emerges out of the fractal geometry and is independent of specific density profile of individual clumps.
3. The model predicts a scale free power spectrum of the rotation velocity fluctuations which can be observationally verified.
4. The model also provides some plausible explanation of the observed intrinsic difference between the dark matter halo density profile of normal galaxies and dark matter dominated low mass dwarf galaxies and low surface brightness galaxies.

We are grateful to Rajaram Nityananda for many useful comments on an earlier version of this paper. We thank Susmita Chakravorty, Aritra Basu, Sanjay Bhatnagar, Abhirup Datta, Prasun Dutta, Sanhita Joshi and Chandreyee Sengupta for helpful discussions. We are also grateful to the anonymous referee for useful comments and for prompting us into substantially improving this paper. NR is a Jansky Fellow of the National Radio Astronomy Observatory (NRAO). This research was supported by the NRAO. The NRAO is a facility of the National Science Foundation (NSF) operated under cooperative agreement by Associated Universities, Inc. (AUI).

Disclaimer: This is an author-created, un-copyedited version of an article accepted for publication in the Astrophysical Journal. IOP Publishing Ltd is not responsible for any errors or omissions in this version of the manuscript or any version derived from it. The definitive publisher authenticated version will be available online at <http://iopscience.iop.org/>.

REFERENCES

- Begeman K. G., Broeils A. H., Sanders R. H., 1991, MNRAS, 249, 523
 Bekenstein J., Milgrom M., 1984, ApJ, 286, 7
 Bertone G., Hooper D., Silk J., 2005, Physics Reports, 405, 279
 Brownstein J. R., Moffat J. W., 2006, MNRAS, 367, 527
 Burkert A., 1995, ApJ, 447, L25
 Burkert A. M., D’Onghia E., 2004, Penetrating Bars through Masks of Cosmic Dust: the Hubble Tuning Fork Strikes a New Note, ed. D. L. Block et al. (Dordrecht: Kluwer), 341
 Chakrabarti S., Blitz L., 2009, MNRAS, 399, L118
 Chen J., 2009, A&A, 498, 49
 Clowe D., Bradač M., Gonzalez A. H. et al., 2006, ApJ, 648, L109
 de Blok W. J. G., 2002, A&A, 385, 816
 de Blok W. J. G., 2005, ApJ, 634, 227
 de Blok W. J. G., 2007, in Island Universe, ed. R. S. de Jong (Dordrecht: Springer), 89
 Dutta P., Roy N., Majumdar S., 2010 (in preparation)
 Elahi P. J., Thacker R. J., Widrow L. M., Scannapieco E., 2009a, MNRAS, 395, 1950
 Elahi P. J., Widrow L. M., Thacker R. J., 2009b, Physical Review D, 80, 123513
 El-Zant A., Hoffman Y., Primack J., Combes F., Shlosman I., 2004, ApJ, 607, L75
 Faber S. M., Jackson R. E., 1976, ApJ, 204, 668
 Fahr H. J., 1990, A&A, 236, 86

- Fukushige T., Makino J., 2001, *ApJ*, 557, 533
- Gao L., White S. D. M., Jenkins A., Stoehr F., Springel V., 2004, *MNRAS*, 355, 819
- Giocoli C., Tormen G., van den Bosch F. C., 2008, *MNRAS*, 386, 2135
- Haynes M. P., Hogg D. E., Maddalena R. J., Roberts M. S., van Zee L., 1998, *AJ*, 115, 62
- Jing Y. P., 2000, *ApJ*, 535, 30
- Jog C. J., Combes F., 2009, *Phys. Rep.*, 471, 75
- Keeton C. R., Moustakas L. A., 2009, *ApJ*, 699, 1720
- Klypin A., Kravtsov A. V., Valenzuela O., Prada F., *ApJ*, 1999, 522, 82
- Knebe A., Libeskind N. I., Knollmann S. R., Yepes G., Gottlöber S., Hoffman Y., 2010, *MNRAS*, 405, 1119
- Kuzio de Naray R., McGaugh S. S., de Blok W. J. G., 2008, *ApJ*, 676, 920
- Ludlow A. D., Navarro J. F., Springel V., Jenkins A., Frenk C. S., Helmi A., 2009, *ApJ*, 692, 931
- Madau P., Diemand J., Kuhlen M., 2008, *ApJ*, 679, 1260
- Mandelbrot B., 1983, *The Fractal Geometry of Nature*, W.H. Freeman, New York
- Massey R., Rhodes J., Ellis R. et al., 2007, *Nature*, 445, 286
- Milgrom M., 1983, *ApJ*, 270, 365
- Moore B., Ghigna, S., Governato F. et al., 1999, *ApJ*, 524, L19
- Navarro J. F., Frenk C. S., White S. D. M., 1996, *ApJ*, 462, 563
- Navarro J. F., Frenk C. S., White S. D. M., 1997, *ApJ*, 490, 493
- Pinzke A., Pfrommer C., Bergström L., 2009, *Physical Review Letters*, 103, 181302
- Richter O.-G., Sancisi R., 1994, *A&A*, 290, L19
- Romano-Díaz E., Shlosman I., Heller C. H., Hoffman Y., 2008, *ApJ*, 685, L105
- Romano-Díaz E., Shlosman I., Heller C. H., Hoffman Y., 2009, *ApJ*, 702, 1250
- Romano-Díaz E., Shlosman I., Hoffman Y., Heller C. H., 2010, *ApJ*, 716, 1095
- Rubin V. C., Ford Jr. W. K., 1970, *ApJ*, 159, 379
- Rubin V. C., Ford Jr. W. K., 1980, *ApJ*, 238, 471
- Saha K., Levine E. S., Jog C. J., Blitz L., 2009, *ApJ*, 697, 2015
- Sanders R. H., 1986, *MNRAS*, 223, 539
- Sanders R. H., 1997, *ApJ*, 480, 492
- Shlosman I., 2010, *Galaxy Evolution: Emerging Insights and Future Challenges* (ASP Conf. Ser. 419), ed. S. Jogee et al., 39
- Sofue Y., 1996, *ApJ*, 458, 120
- Sofue Y., Rubin V., 2001, *ARA&A*, 39, 137
- Sommer-Larsen J., Dolgov A., 2001, *ApJ*, 551, 608
- Sommer-Larsen J., Gelato S., Vedel H., 1999, *ApJ*, 519, 501
- Spano M., Marcelin M., Amram P. et al., 2008, *MNRAS*, 383, 297
- Springel V., Wang J., Vogelsberger M., Ludlow A., Jenkins A., Helmi A., Navarro J. F., Frenk C. S., White S. D. M., 2008, *MNRAS*, 391, 1685
- Swaters R. A., Schoenmakers R. H. M., Sancisi R., van Albada T. S., 1999, *MNRAS*, 304, 330
- Taylor J. E., Navarro J. F., 2001, *ApJ*, 563, 483
- Vegetti S., Koopmans L. V. E., 2009, *MNRAS*, 400, 1583
- Weinberg D. H., Colombi S., Davé R., Katz N., 2008, *ApJ*, 678, 6
- Xu D. D., Mao S., Wang J., Springel V., Gao L., White S. D. M., Frenk C. S., Jenkins A., Li G., Navarro J. F., 2009, *MNRAS*, 398, 1235
- Zemp M., Diemand J., Kuhlen M. et al., 2009, *MNRAS*, 394, 641
- Zhao H., 1996, *MNRAS*, 278, 488